The Journal of the Astronautical Sciences, Vol. 38, No. 4, October-December 1990, pp. 531-556

Flexibility Effects on the Control System Performance of Large Scale Robotic Manipulators

Sabri Cetinkunt[1] and Wayne J. Book[2]

Abstract

Structural flexibility of robotic manipulators becomes significant and limits the performance of a control system when manipulators are large structures, manipulating on large payloads, and/or operating at high speeds. The question of when a manipulator can be considered rigid or must be considered flexible is studied as a function of manipulator dynamics and task characteristics. Results are interpreted in simple quantitative forms which can be used as design and analysis tools to decide whether or not the manipulator flexibility will be a significant factor for a given task condition. The limitations imposed by the manipulator flexibility on the joint variable feedback control system performance is determined using linear and nonlinear methods. The closed loop eigenstructure behavior of finite dimensional models under joint variable feedback is studied and results are compared with the previously reported results.

I. Introduction

The state of the art in robot manipulator control is that manipulators are assumed to be rigid structures. Controllers that use joint variable feedback information are designed based on that assumption. Robot motion speeds, therefore, must be restricted to a relatively low speed range in order to keep the rigidity assumptions valid and achieve the expected controller performance. The speed of robotic manipulators is limited by the structural vibration characteristics of links and drive system. For instance, as a rule of thumb Paul [1] and Luh [2] suggest that the closed loop system bandwidth of independent joint controllers should be less than one half of the lowest natural frequency of the manipulator system. In search of improving performance, Book et al. [3] investigated the effects of link flexibilities on the closed loop dynamics. They also have provided simple design rules based on the explicit study of structural flexibility effects.

It has become clear that when the closed loop bandwidth is greater than a certain limit, which is determined by the manipulator flexibility, the performance

[1]Assistant Professor, Department of Mechanical Engineering, University of Illinois at Chicago, Chicago, IL 60680.

[2]Professor, The George W. Woodruff School of Mechanical Engineering, Georgia Institute of Technology, Atlanta, GA 30332.

deteriorates and structural vibrations become very significant. If the closed loop bandwidth is well below such a critical limit, the flexibility can be ignored and the rigid manipulator assumptions are satisfactory. The critical limit is determined by the inertial and structural properties of the manipulator and the payload. For a given manipulator, the critical speed range varies as the payload changes from one task to another. The range of variations is very wide in space robotics applications where very large payloads are anticipated. The speed limit for traditional manipulator control systems must be set for the worst possible case, leading to further underutilization of performance.

In space applications, the structure of manipulators is different than the traditional industrial manipulators. Industrial manipulators are designed very bulky to provide high rigidity which in turn increases the bandwidth limit set by the flexibility. Similar bulky structures can not be afforded in space. Space robots must be large structures with big workspace, and long reach. They manipulate on huge payloads (Fig. 1). The large structure and large payload character of space robots generates serious concerns over the structural vibration even for very slow motions. Motion control algorithms analogous to industrial manipulators will not be satisfactory. The flexibility of the robot must be accounted for in the design of controllers and motion planning algorithms. Dynamics and control studies of flexible manipulators have been concentrated on a single beam [4, 5, 6, 7]. The single beam is modeled as a Bernoulli-Euler beam and infinite dimensional vibration coordinates are truncated with a finite number of mode shapes. The model order reduction to finite order readily allows the application of finite dimensional linear control theory to the control problem. The price paid for this simplification is the error caused by the interaction between the controller, the controlled dynamics and the truncated dynamics (control and observation spillover problem [7]).

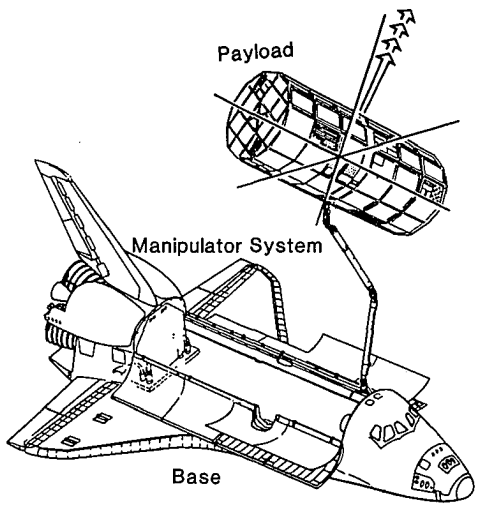

FIG. 1. A Large Scale Robotic Manipulator Application in Space.

Studies on multi-link flexible manipulators have been primarily concentrated on dynamics. Little work has been done in fine motion control, almost none in the general gross motion control aspects. Sunada and Dubowsky [8, 9] developed a Lagrangian-finite-element based method to model the small vibration dynamics about known nominal joint motions. This method ignored the coupling effects of flexible vibrations on the joint motion. Shabana and Wehage [10] included the coupling between joint and flexible coordinates and presented a general method to derive a full nonlinear dynamic model of a flexible system. Naganathan and Soni [11] studied the link flexibility effects on the dynamics of a two link manipulator. Shahinpoor and Maghdani [12] derived combined link and joint flexibility representation of a two-link example. A two link manipulator with flexible drive system are experimentally studied by Hollars and Cannon [13]. Book [14] took a different approach in dynamic modeling and presented a very general method based on the Lagrangian-assumed modes method. Cetinkunt and Book [15, 16] developed symbolic modeling algorithms based on the method of [14].

Book, Neto, and Whitney [3], Book and Majette [17] have studied the performance of joint variable feedback controllers on flexible arms for fine motions where nonlinear effects can be neglected. Therefore, the results can not be extended to high speed gross motions where nonlinear effects become significant. The concern over the flexibility becomes very important in large robot structures and high speed manipulation. The significance of flexibility and the best performance of joint variable feedback controllers must be determined for general motions of the manipulator as the fundamental step towards improving the performance of space and industrial robots.

The remaining part of this paper is organized as follows. Section II states the problem discussed in this paper in a precise manner. Section III outlines the mathematical modeling of flexible manipulator dynamics using the Lagrangian-assumed-modes method, and describes the model on which the following analysis are performed. The analysis and control methods used are described in Section IV. The results are presented and discussed in Section V. The conclusions of the work are in Section VI.

II. The Problem Statement

It is not yet clearly understood when the flexibility becomes significant and when one must be concerned with flexible vibrations. Therefore, very conservative rule of thumb design rules are suggested to guarantee that the flexibility will not be significant even in the worst possible cases. This results in the underutilization of the capabilities of the robot. Book supported his design rules by explicit analysis of flexibility in fine motion [3, 17]. However, results cannot be generalized to fast gross motions where dynamic nonlinear effects become significant relative to other dynamic forces.

The *first objective* of this work is to determine when a manipulator must be considered flexible and when it can be considered rigid. The *second objective* is to study the best performance that can be achieved by control algorithms using joint position and velocity feedback, for a given manipulator with structural flexibility.

The conditions at which flexibility becomes significant and the conditions at which the best performance is achieved are not totally independent of each other. Now, we will clarify the difference between them. We will designate that the arm flexibility starts to become significant when the behavior of the flexible arm starts to deviate from the behavior of an equivalent rigid arm under the same conditions. The behavior comparison will be quantified using the root locus analysis in fine motion, and the time domain simulations in high speed gross motions. Here, an equivalent rigid arm means that it has the same geometric and inertial properties, but has no structural flexibility.

The best performance of a joint variable feedback controller in fine motion is defined as the highest closed loop bandwidth possible with damping ratios more than 0.707. In gross motion where nonlinear terms are significant the concept of bandwidth is no longer well defined. However, in the context of model reference control, the bandwidth of the reference model with step input can be used as the measure of performance.

The significance of solving these problems is two-fold: first, for a given manipulator, one can determine the range of the closed loop bandwidth for which the arm flexibility can be safely ignored, and the range where the flexibility of the arm must be taken into account. Second, the best possible performance of joint variable feedback controllers can be determined and the designer may not attempt to achieve higher performances. Furthermore, this result can be used as a reference to evaluate the relative merits of more sophisticated control algorithms employing sensory information about the flexible behavior of the arm in addition to the joint variables.

III. Mathematical Model of Flexible Manipulator Dynamics

The first step in dynamic modeling of any mechanical system is to establish the coordinate frames so that the fundamental vector quantities position, velocity and acceleration of any element of the system can be defined. Consider the kinematic structure of Fig. 2, representing an n-link manipulator with flexible links. Let us define the coordinate system as follows: O_oXYZ is fixed to the base (global coordinate frame); O_ixyz is fixed to the base of link i; and $O_i'xyz$ is fixed to the end of link i. If the links were rigid, $O_i'xyz$ coordinates would not be needed. The position vector of any point on link i with respect to O_ixyz coordinates, ${}^i\mathbf{h}(x_i)$, can be expressed as;

$$ {}^i\mathbf{h}(x_i) = [x_i, 0, 0, 1]^T + [w_{xi}(x_i, t), w_{yi}(x_i, t), w_{zi}(x_i, t), 0]^T \tag{3.1} $$

where $w_{xi}(x_i, t)$, $w_{yi}(x_i, t)$, $w_{zi}(x_i, t)$ are axial and transverse displacements of the element due to arm flexibility in the x, y, z directions, respectively. The dependence of w_{xi}, w_{yi}, and w_{zi} on the spatial variable x_i makes the dynamic order of the system infinite. The resultant dynamic model would consist of nonlinear, coupled ordinary and partial differential equations. In general, the distributed form of the links is approximated by a finite series consisting of assumed spatial variable-dependent shape functions multiplied by time-dependent generalized coordinates:

$$ w_{\beta i}(x_i, t) = \sum_{j=1}^{n_{\beta i}} \phi_{\beta ij}(x_i)\, \delta_{\beta ij}(t); \qquad \beta : x, y, z \tag{3.2} $$

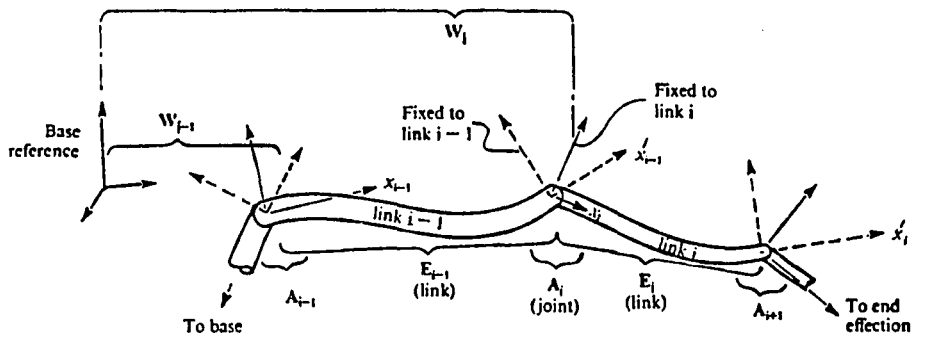

FIG. 2. Kinetic Description of a General Serial Manipulator Structure with Flexible Links.

where $n_{\beta i}$ is the number of shape functions considered in the approximation, $\phi_{\beta ij}(x_i)$'s are shape functions assumed, and $\delta_{\beta ij}(t)$'s are the generalized coordinates associated with the flexible behavior. With the approximation (3.2), the dynamic order of the system is reduced from infinity to a finite number, and thus the dynamic equations will be in ordinary differential equation form. The controller will be designed based on the truncated finite dimensional model, then applied to the actual system which is infinite dimensional. The truncated part of the dynamics, which is ignored for the controller design purposes, will interact with the controller in actual implementation and result in errors by two mechanisms: 1. The truncated dynamics will be excited through the coupling from the controller and the controlled dynamics; 2. Because of the existence of the truncated part, originally targeted closed loop dynamics will not be quite exactly achieved [17, 7]. Nonetheless, any finite dimensional controller design based on finite dimensional models will have these problems.

Finally, to describe the position vector with respect to base coordinate frame, ${}^o\mathbf{h}(x_i)$, let ${}^oW_i$ be the (4×4) homogeneous transformation matrix describing the position and orientation of O_ixyz with respect to O_oXYZ, then

$$ {}^o\mathbf{h}(x_i) = {}^oW_i\,{}^i\mathbf{h}(x_i) \tag{3.3} $$

$$ {}^oW_i = {}^oW_{i-1}E_{i-1}A_i \tag{3.4} $$

where A_i is the joint transformation matrix and E_{i-1} is the flexible link transformation (Fig. 2) matrix. Once the kinematic description is complete, and the number of mode shapes used for flexible members is decided upon, the dynamic model can be developed using the Lagrangian-assumed-modes method. An efficient symbolic modeling algorithm is developed in [16] which allows one to obtain symbolic equations of motion explicitly and does not require the specification of mode shapes at the modeling level. After dynamic equations are obtained symbolically, the mode shapes can be chosen from the admissible class as one input set of the simulation.

The derivation of a dynamic model involves obtaining the kinetic and potential energy of each element of the system, then taking the necessary derivatives with respect to generalized coordinates and time, as required by the Lagrangian formulation. Details of the modeling algorithm are found in [15, 16, 18]. Letting

the generalized coordinates $\mathbf{q}$ of the system be grouped as $\mathbf{q} = [\theta, \delta]$, the time-domain dynamic model of the manipulator having flexible links can be expressed in general form as,

$$\begin{bmatrix} m_r(\theta,\delta) & m_{rf}(\theta,\delta) \\ m_{rf}^T(\theta,\delta) & m_f(\theta,\delta) \end{bmatrix} \begin{Bmatrix} \ddot{\theta} \\ \ddot{\delta} \end{Bmatrix} + \begin{Bmatrix} f_r(\theta,\dot{\theta},\delta,\dot{\delta}) \\ f_f(\theta,\dot{\theta},\delta,\dot{\delta}) \end{Bmatrix} + \begin{Bmatrix} 0 \\ [K]\delta \end{Bmatrix} + \begin{Bmatrix} g_r(\theta,\delta) \\ g_f(\theta,\delta) \end{Bmatrix} = \begin{bmatrix} I \\ B_m \end{bmatrix} \mathbf{u} \tag{3.5}$$

where: $m_r(\theta, \delta), m_{rf}(\theta, \delta), m_f(\theta, \delta)$ are partitioned elements of the generalized inertia matrix which is always positive definite and symmetric; $f_r(\theta, \dot{\theta}, \delta, \dot{\delta}), f_f(\theta, \dot{\theta}, \delta, \dot{\delta})$, are Coriolis and centrifugal terms which are quadratic in the generalized coordinate velocities $(\dot{\theta}, \dot{\delta})$; $g_r(\theta, \delta), g_f(\theta, \delta)$ are gravitational terms; $[K]$ is the structural stiffness matrix associated with arm flexibility and mode shape functions; and B_m is the input matrix which is a function of mode shapes and defines the actuator coupling to the flexible modes. θ represents the joint angle vector, and δ represents the generalized coordinates associated with the flexible mode shapes, $\mathbf{u}$ represents the effective torque (or force) input vector at the joints.

The equation (3.5) is a highly nonlinear and coupled ordinary differential equation set. This makes the controller synthesis and design problem difficult. Furthermore, experiments indicate that the mode shapes of the beams quickly converge to the mode shapes of a clamped-base beam under joint variable feedback control for even low values of feedback gains of interest [4, 5]. All mode shapes of a clamped-base beam have zero slope at the base, therefore the $B_m = 0$ for the dynamics of flexible manipulators under feedback control. That means the joint variable controller affects the flexible variables through the coupling from joint variables, but not directly. In order to give a clear idea about the complexity of the dynamic model equations for flexible manipulators, we state the following computational results for a two-link, two-joint flexible arm (Fig. 3). The model has six generalized coordinates, two of which are joint variables and four of which are for the representation of flexible motion (two mode shapes for each link). Given $\theta, \dot{\theta}, \delta, \dot{\delta}$, calculation of m_r, m_{rf}, m_f, f_r, f_f, g_r, g_f, $[K]\ \delta$ can be done at the following rate:

1. Computer: VAX-11/750
   a) without floating point accelerator: 7 Hz.
   b) with floating point accelerator: 14 Hz.
2. Eight transputers (T414) configured in parallel computation architecture (estimated value, not fully implemented): 80 Hz.

IV. Linear and Nonlinear Analysis of the Flexibility Effects

The question of when the arm flexibility becomes significant and what limitations it imposes on the performance of joint variable controllers are studied first using linear techniques. Linear analysis results are valid only for the fine motions when nonlinearities are negligible. In order to determine the effect of dynamic nonlinearities (Coriolis and centrifugal forces), linear and nonlinear control algorithms are simulated on the nonlinear model in equation (3.5) for

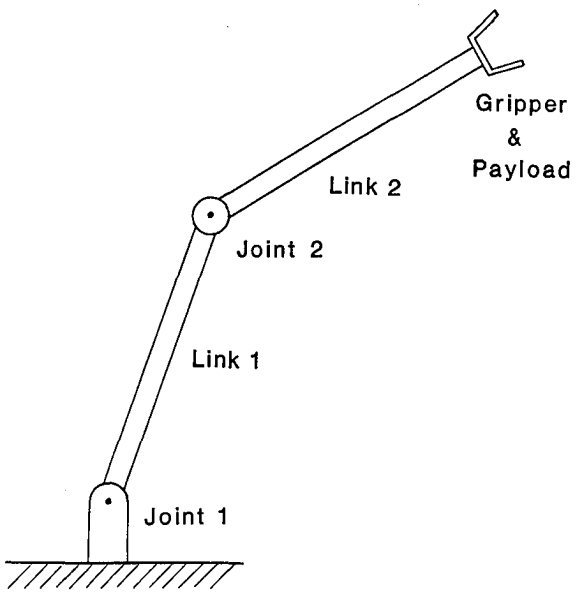

FIG. 3. Two-link Flexible Manipulator Example.

motions where nonlinear effects are larger relative to other dynamic forces of the system, such as inertial and gravitational forces.

IV.1. Linear Analysis

The nonlinear model in equation (3.5) is linearized about a nonlinear configuration, $\mathbf{x}_n = [\theta, \delta, \dot{\theta}, \dot{\delta}] = [\theta_{nominal}, 0, 0, 0]$ and nominal input $\mathbf{u}_n$ which compensates for the nominal gravitational loading. Since nonlinear Coriolis and centrifugal terms are quadratic in $\dot{\theta}, \dot{\delta}$, they drop out upon linearizing about a nominal configuration with nominal values of $\dot{\theta} = \dot{\delta} = 0$.

Let $\theta = \theta_{nominal} + \Delta\theta$, $\delta = \delta_{nominal} + \Delta\delta$, and $\mathbf{u} = \mathbf{u}_{nominal} + \Delta\mathbf{u}$, then the linear dynamic model about the nominal configuration $\mathbf{x}_{nominal} = [\theta_{nominal}, 0, 0, 0]$ is given by equation (4.1),

$$\underbrace{\begin{bmatrix} m_r & m_{rf} \\ m_{rf}^T & m_f \end{bmatrix}_{|(\theta_n,0)}}_{M_{eff}} \begin{Bmatrix} \Delta\ddot{\theta} \\ \Delta\ddot{\delta} \end{Bmatrix} + \underbrace{\begin{bmatrix} \partial g_r/\partial\theta & \partial g_r/\partial\delta \\ \partial g_f/\partial\theta & \partial g_f/\partial\delta + [K] \end{bmatrix}_{|(\theta_n,0)}}_{K_{eff}} \begin{Bmatrix} \Delta\theta \\ \Delta\delta \end{Bmatrix} = \begin{Bmatrix} \Delta\mathbf{u} \\ 0 \end{Bmatrix} \tag{4.1}$$

In compact form, let $\Delta\mathbf{x} = [\Delta\theta, \Delta\delta, \Delta\dot{\theta}, \Delta\dot{\delta}]$, and the linear dynamic model about the given nominal configuration can be expressed as,

$$\Delta\dot{\mathbf{x}} = A\Delta\mathbf{x} + B\Delta\mathbf{u} \tag{4.2}$$

where

$$A = \begin{bmatrix} 0 & I \\ -M_{eff}^{-1}K_{eff} & 0 \end{bmatrix}, \qquad B = \begin{bmatrix} 0 \\ -M_{eff}^{-1}(I) \end{bmatrix} \tag{4.3}$$

The closed loop eigenstructure of the linear model under linear joint variable feedback controllers is studied as a function of feedback gains. The linear joint variable feedback controller has the general form

$$\Delta \mathbf{u} = -[K_{ij}]\Delta\theta - [C_{ij}]\Delta\dot{\theta} \tag{4.4}$$

For independent joint control;

$$[K_{ij}] = \text{diag}\{k_{ii}\}$$
$$[C_{ij}] = \text{diag}\{c_{ii}\}$$

For decoupled joint control;

$$[K_{ij}] = m_r(\theta_{nominal}, 0)\ \text{diag}\{k_{ii}\}$$
$$[C_{ij}] = m_r(\theta_{nominal}, 0)\ \text{diag}\{c_{ii}\}$$

Independent joint control results are presented here in order to compare with the previously reported ones. Position and velocity feedback gains of joint 1, (k_{11}, c_{11}), are set to very high values in order to force joint 1 to behave like a clamped base. The locus of closed loop eigenvalues are studied as a function of joint 2 feedback gains, k_{22}, c_{22} (Fig. 5). The finite dimensional linear model should be able to predict at least the dominant behavior of the closed loop dynamics of the infinite dimensional actual system, despite the errors introduced due to truncated dynamics. Otherwise the truncated finite dimensional model would not be of any value.

By comparing the root locus behavior of a given flexible manipulator with that of an equivalent rigid manipulator, the conditions at which flexibility becomes significant and the range of conditions where the flexibility can be ignored can be determined. The study of dominant behavior of closed loop eigenvalues will determine the best possible performance in fine motion.

IV.2. Nonlinear Analysis

The effect of nonlinear Coriolis and centrifugal forces on the significance of flexibility and the best performance of joint variable feedback controllers are studied using high speed motion simulations. The fundamental challenge in the control of space and industrial robots is to provide high speed, high precision motions despite large payload variations and external disturbances. In the authors' opinion, extensive research in the past decade has shown that adaptive control methods are potentially more promising to meet that challenge than the non-adaptive control methods. Therefore, the nonlinearity effects will be studied with an adaptive controller in the closed loop.

The main objective is to study the effect of nonlinearities on the flexibility problem, not the adaptive controller. Here, the adaptive control algorithm is directly stated. The design details and analysis of the adaptive controller can be found in [18].

Let us call $\mathbf{x}_\theta = [\theta, \dot{\theta}]$. The adaptive control algorithm is given by, (Fig. 4),

$$\mathbf{u} = -K_{pn}\mathbf{x}_\theta + K_{un}\mathbf{u}_m + \Delta K_p(e,t)\mathbf{x}_\theta + \Delta K_u(e,t)\mathbf{u}_m \tag{4.5}$$

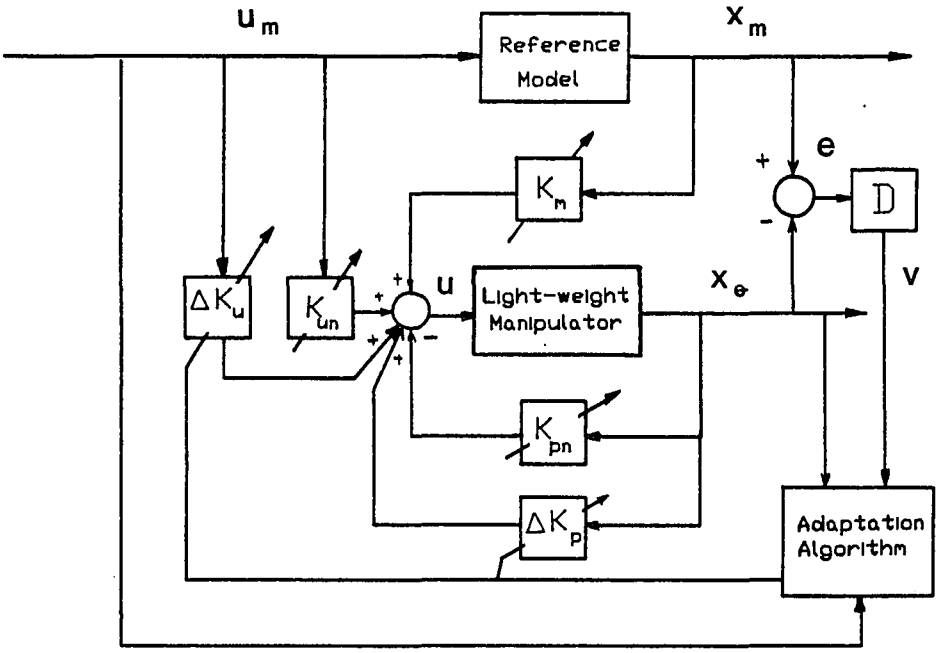

FIG. 4. Generalized Inertia Matrix Based Adaptive Model Following Control System Block Diagram.

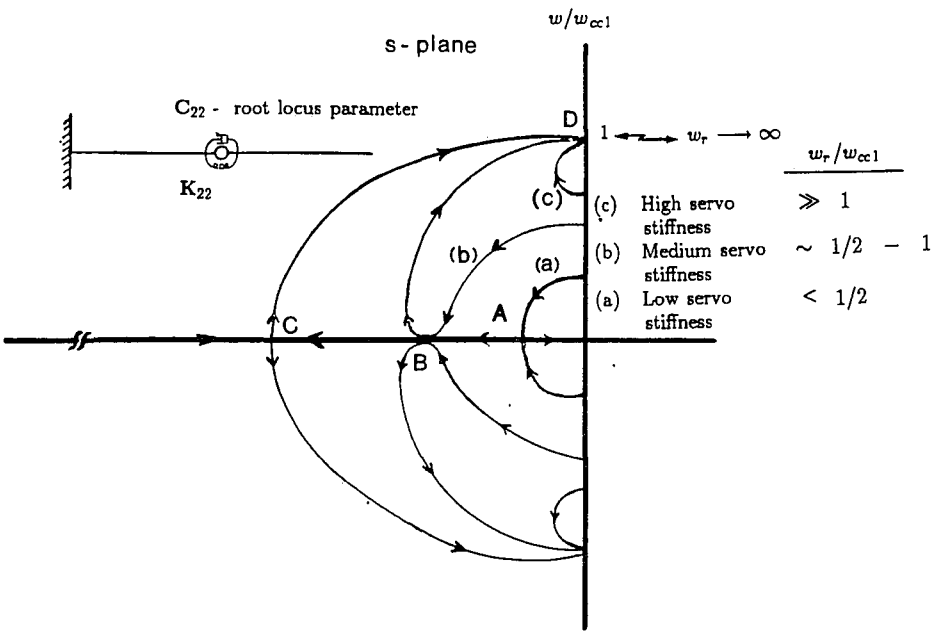

FIG. 5. Illustration of Joint Variable Feedback Controller Limitations Due to Arm Flexibility.

where;

$$K_{pn} = m_r(\theta, \delta_{st})[[k_{ii}], [c_{ii}]] \tag{4.6a}$$

$$K_{un} = m_r(\theta, \delta_{st}) \tag{4.6b}$$

$$\Delta K_p = \int_0^t p_{pi} m_r(\theta_o, \delta_{st}) \nu \mathbf{x}_\theta^T \, d\tau \tag{4.6c}$$

$$\Delta K_u = \int_0^t p_{ui} m_r(\theta_o, \delta_{st}) \nu \mathbf{u}_m^T \, d\tau \tag{4.6d}$$

$[k_{ii}]$ and $[c_{ii}]$ are the reference model dynamic components chosen by the designer, δ_{st} is the vector of static deflection values of flexible modes. Here, the reference model is chosen as a decoupled linear system of the form

$$\begin{bmatrix} \dot{\theta}_m \\ \ddot{\theta}_m \end{bmatrix} = \begin{bmatrix} 0 & I \\ [-k_{ii}] & [-c_{ii}] \end{bmatrix} \begin{bmatrix} \theta_m \\ \dot{\theta}_m \end{bmatrix} + \begin{bmatrix} 0 \\ [k_{ii}] \end{bmatrix} \mathbf{u}_m \tag{4.7}$$

The response of the reference model, $\theta_m(t)$, to the commanded input, $\mathbf{u}_m(t)$, is the desired joint response. The reference model dynamics affect the control through equations (4.6a, c, d). Using δ_{st} in the control algorithm does not require real-time feedback information about the flexible states. Therefore, the controller is still a joint variable feedback control algorithm. The use of δ_{st} as opposed to 0 (zero) for the flexible modes is more accurate and improves the decoupled control of the flexible manipulator without imposing any significant implementation difficulty. ν is the filtered tracking error e (Fig. 4). p_{pi} and p_{ui} are arbitrary, scalar adaptive controller design parameters affecting the convergence rate of the adaptive control system and the transient response of the closed loop system. The design advantages, performance improvements, and stability aspects of this algorithm are discussed in detail in [18]. In order to see the effect of dynamic nonlinearities, the closed loop system is simulated for two classes of motions: first, slow motions where nonlinear forces are small, and secondly, fast motions where nonlinear forces are significantly larger or of the same magnitude as the other dynamic forces.

V. Results and Discussion

V.1 Linear Analysis Results and Discussion

Let ω_{cc1} be the lowest structural natural frequency of the arm when both joints are clamped (k_{11} and $k_{22} \rightarrow \infty$, and $c_{11} = c_{22} = 0.$, Fig. 5). Consider an equivalent rigid manipulator, with the same inertial and geometric properties of the flexible manipulator except that it is rigid. The rigid system with first joint clamped will be a second order mass-spring system with feedback gains $k_{22} \neq 0$ and $c_{22} = 0$. Let ω_{r1} be the undamped natural frequency of the rigid system for a given position feedback value.

It is the ratio of ω_{r1}/ω_{cc1} that determines the significance of flexibility and the dominant behavior of the closed loop system. In the rigid arm case it is possible to achieve arbitrarily large closed loop bandwidth (undamped natural frequency) by increasing k_{22}, for $\omega_{r1} = \sqrt{(k_{22}/(J_{o2})_{eff}}$, where $(J_{o2})_{eff}$ is the effective moment

of inertia of link 2 and payload about the joint 2 axis of rotation. However when the same controller is applied to the flexible arm, the closed loop bandwidth ω_{f1} will be definitely smaller than ω_{cc1}; that is as $k_{22} \to \infty$, $\omega_{f1} \to \omega_{cc1}$ (Fig. 5). If the servo stiffness is low relative to arm flexibility, that is if $\omega_{r1}/\omega_{cc1} \ll \frac{1}{2}$, the locus of closed loop eigenvalues is indistinguishable from that of the rigid arm as c_{22} increases. However, if velocity feedback c_{22} is further increased to too large values, the result is to stiffen the joint. One dominant eigenvalue meets with another and breaks away from the real axis converging to the ω_{cc1} on the imaginary axis as c_{22} increases (Figs. 5 and 6). In the rigid arm case this phenomenon does not exist for any value of feedback gains. The root locus analysis is done as a function of c_{22} for many other values of ω_{r1}/ω_{cc1} (Figs. 6, 7, 8). It is seen that above a critical value of the ω_{r1}/ω_{cc1} ratio, the dominant eigenvalues are no longer able to reach the real axis (Fig. 5, curve b, Fig. 7f). Physically that means that if the joint position control is too stiff relative to the arm flexibility, it is not possible to provide well damped dominant modes no matter how large the velocity feedback is.

For a given manipulator and payload, ω_{cc1} is determined by the geometric, inertial and structural flexibility properties. If a joint variable controller attempts closed loop bandwidth larger than $(\frac{1}{2})\omega_{cc1}$, then the flexibility of the arm will be significant. Otherwise the flexibility of the arm can be reasonably ignored and the controller can be designed as if the arm were rigid (Figs. 5, 6, 7, 8).

The *best* performance of a joint variable feedback controller is defined here as the highest possible dominant eigenvalues with damping ratio of 0.707 or more. As shown in Fig. 7f, approximately $(\frac{2}{3})\omega_{cc1}$ closed loop bandwidth value can be

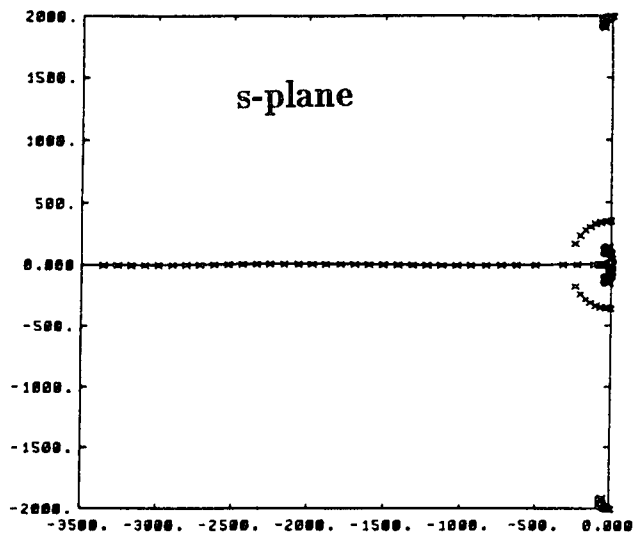

(a)

FIG. 6. Locus of Closed Loop Eigenvalues as a Function of Joint 2 Velocity Feedback Gain: Low Servo Stiffness Case (Each Figure is a Closer Look of the Previous Figure).

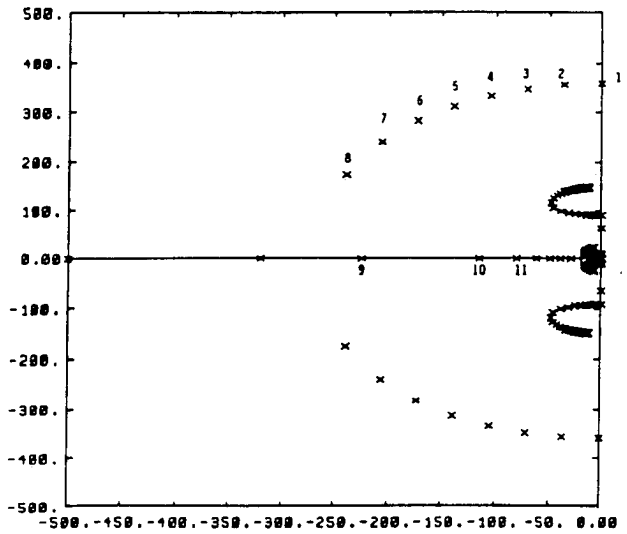

(b)

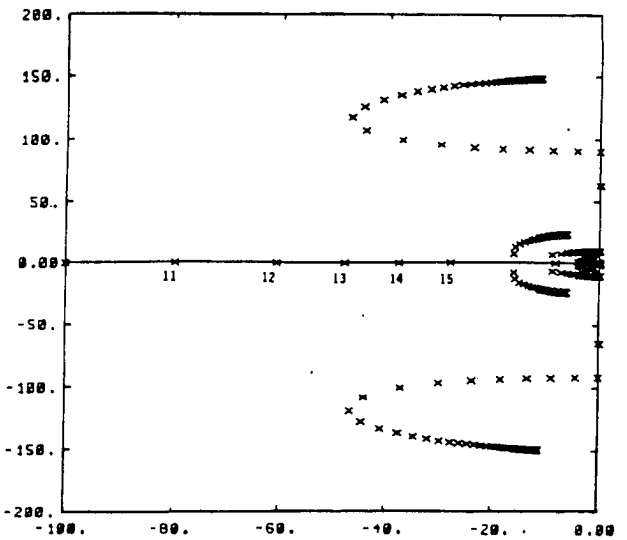

(c)

FIG. 6. Cont. Locus of Closed Loop Eigenvalues as a Function of Joint 2 Velocity Feedback Gain: Low Servo Stiffness Case (Each Figure is a Closer Look of the Previous Figure).

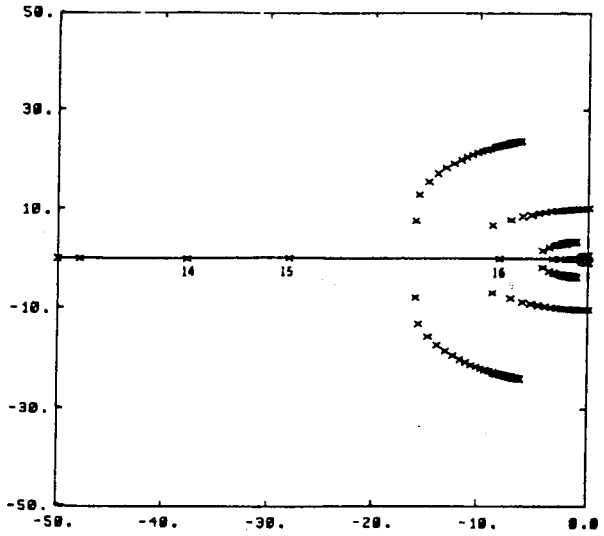

(d)

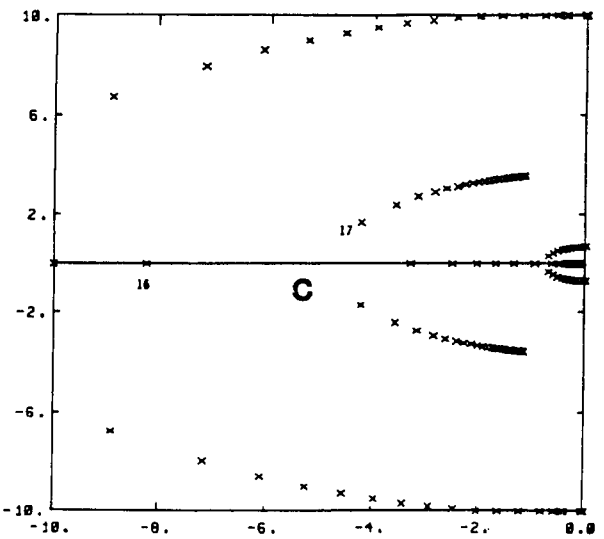

(e)

FIG. 6. Cont. Locus of Closed Loop Eigenvalues as a Function of Joint 2 Velocity Feedback Gain: Low Servo Stiffness Case (Each Figure is a Closer Look of the Previous Figure).

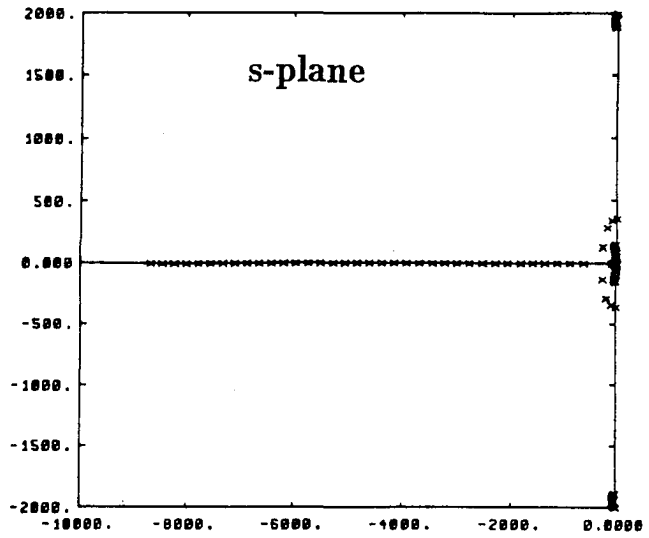

(a)

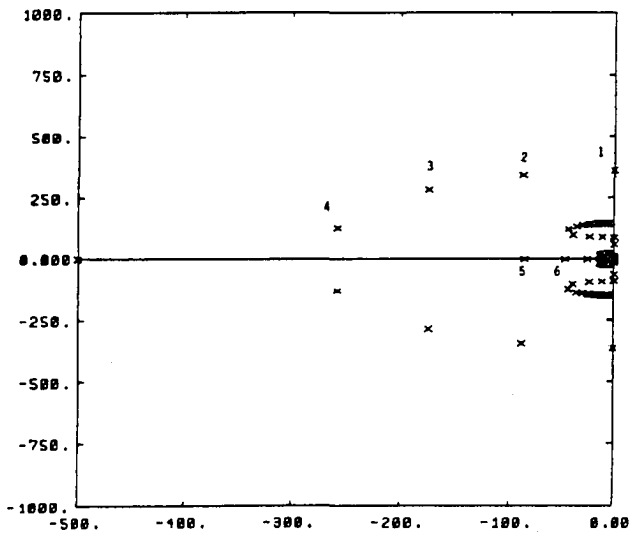

(b)

FIG. 7. Locus of Closed Loop Eigenvalues as a Function of Joint 2 Velocity Feedback Gain: Medium Servo Stiffness Case (Each Figure is a Closer Look of the Previous Figure).

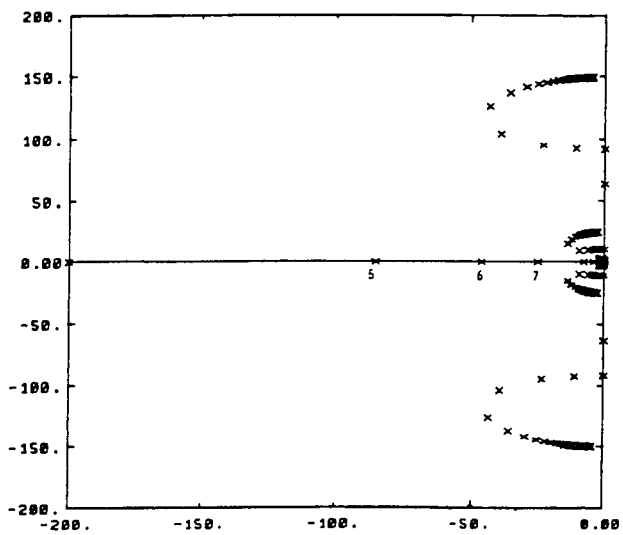

(c)

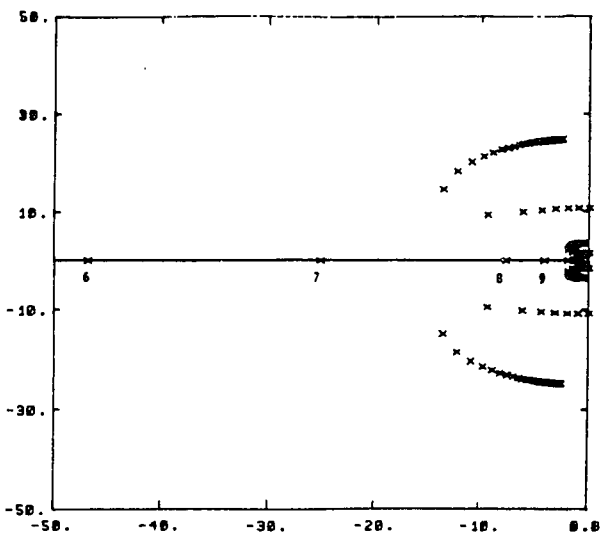

(d)

FIG. 7. Cont. Locus of Closed Loop Eigenvalues as a Function of Joint 2 Velocity Feedback Gain: Medium Servo Stiffness Case (Each Figure is a Closer Look of the Previous Figure).

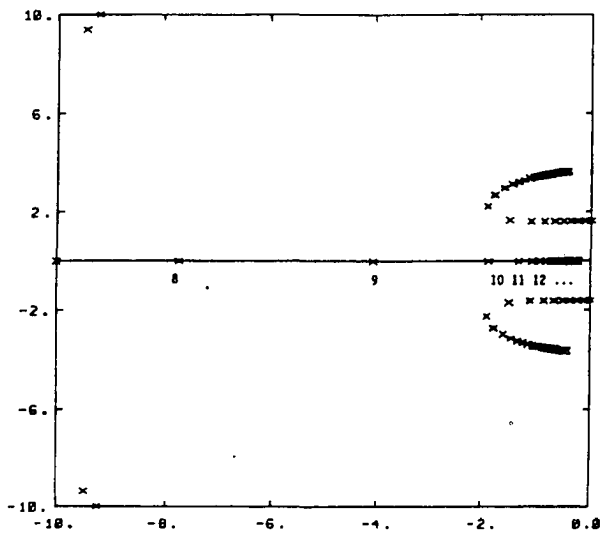

(e)

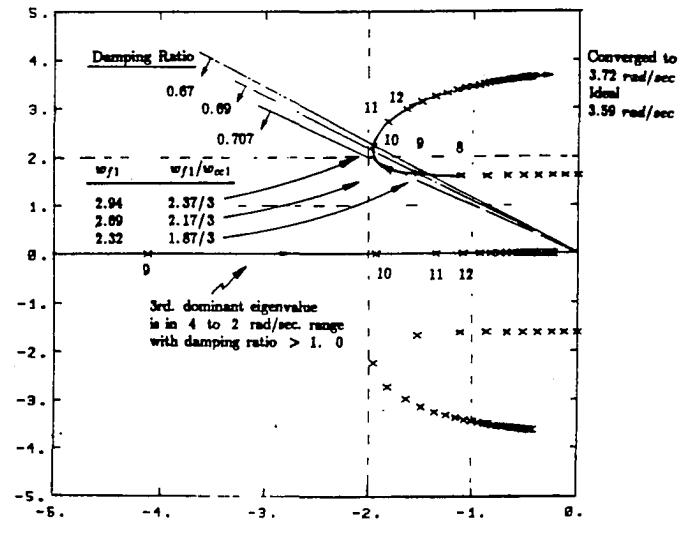

(f)

FIG. 7. Cont. Locus of Closed Loop Eigenvalues as a Function of Joint 2 Velocity Feedback Gain: Medium Servo Stiffness Case (Each Figure is a Closer Look of the Previous Figure).

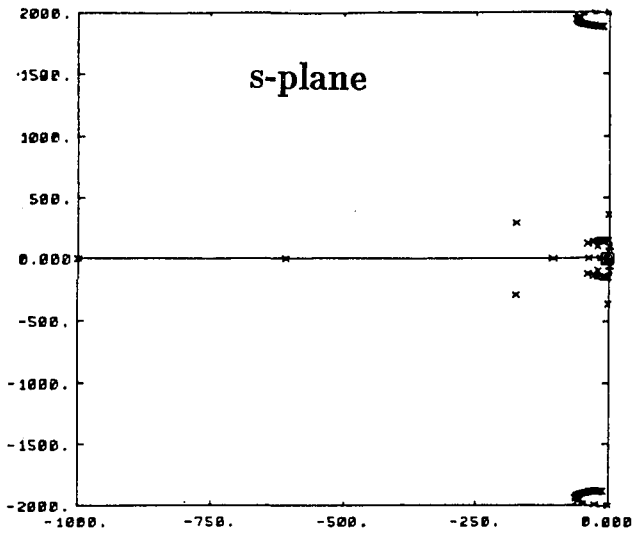

(a)

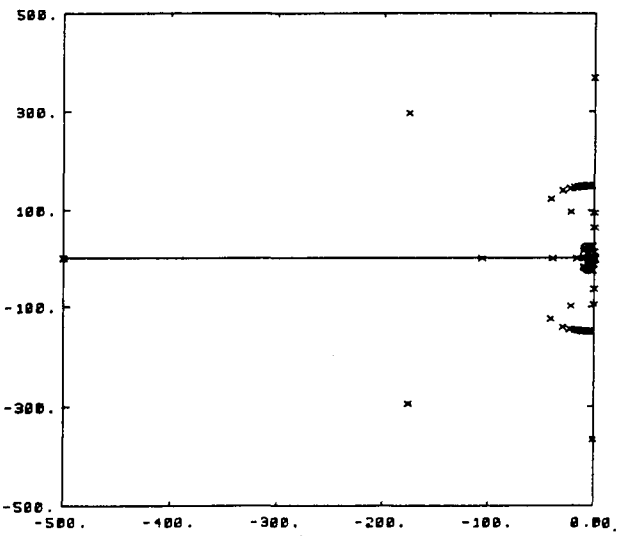

(b)

FIG. 8. Locus of Closed Loop Eigenvalues as a Function of Joint 2 Velocity Feedback Gain: High Servo Stiffness Case (Each Figure is a Clsoer Look of the Previous Figure).

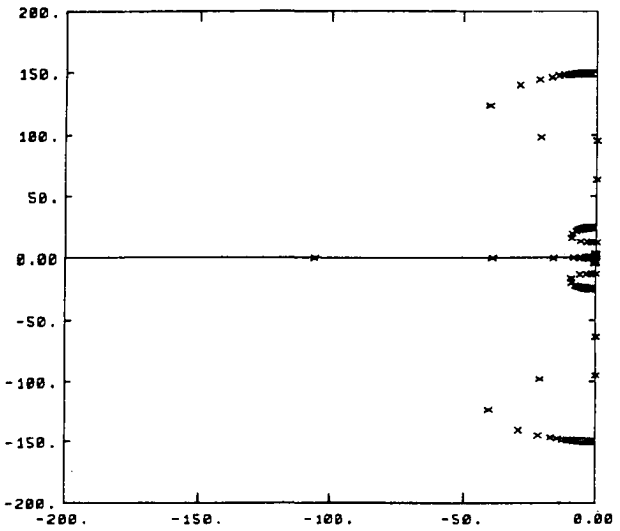

(c)

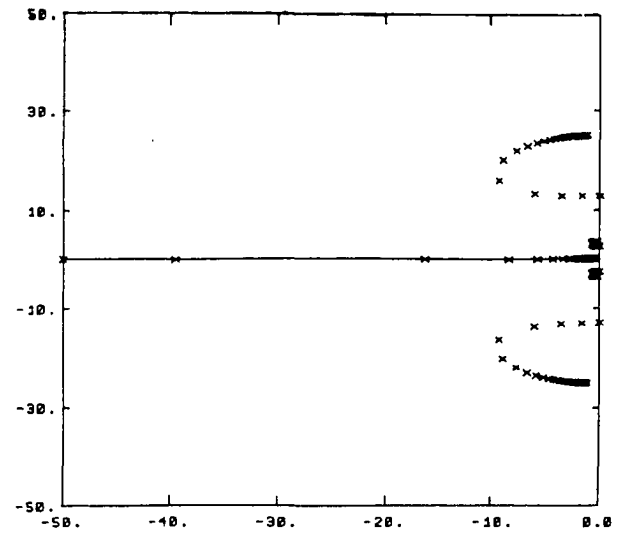

(d)

FIG. 8. Cont. Locus of Closed Loop Eigenvalues as a Function of Joint 2 Velocity Feedback Gain: High Servo Stiffness Case (Each Figure is a Closer Look of the Previous Figure).

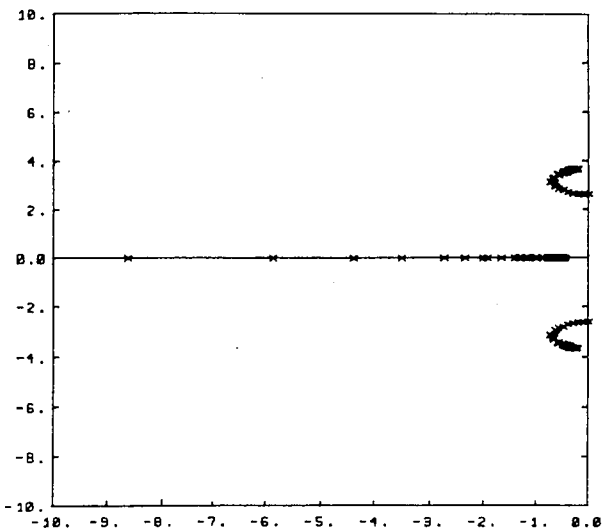

(e)

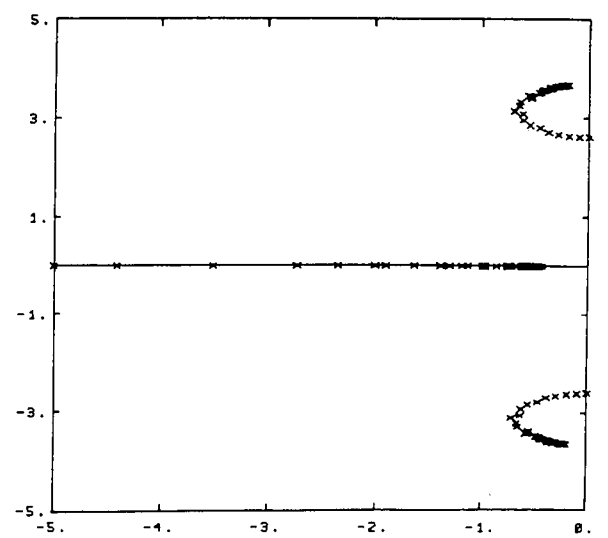

(f)

FIG. 8. Cont. Locus of Closed Loop Eigenvalues as a Function of Joint 2 Velocity Feedback Gain: High Servo Stiffness Case (Each Figure is a Closer Look of the Previous Figure).

achieved by appropriate choice of joint variable feedback gains k_{22} and c_{22}. It is important to note that the dominant eigenvalue locations are very sensitive to the variation of joint velocity feedback gain around the best solution (Fig. 7f, between each point velocity feedback gain is incremented a constant amount).

Based on our definition of best performance, a manipulator is best utilized if its speeds are high to the point where the flexibility becomes significant, yet does not pose a problem due to well damped dominant modes. The results presented here, concerning the flexibility significance and dominant closed loop dynamics, agree very well with the results based on infinite dimensional models of [3].

V.2. Nonlinear Analysis Results

Figure 10 shows the response of the manipulator with adaptive controller to the desired slow motion. Two different adaptive control results are shown for *slow* and *fast* adaptation, referring to small and large values of the adaptation parameters p_{pi} and p_{ui}. The appropriate values for these parameters are found by

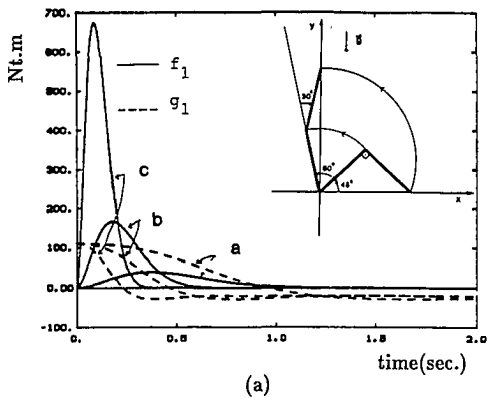

(a)

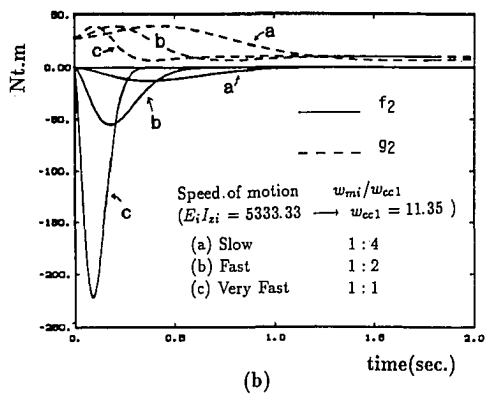

(b)

FIG. 9. Relative Importance of Nonlinear (Coriolis and Centrifugal) Forces and Gravitational Forces Along Different Motions.

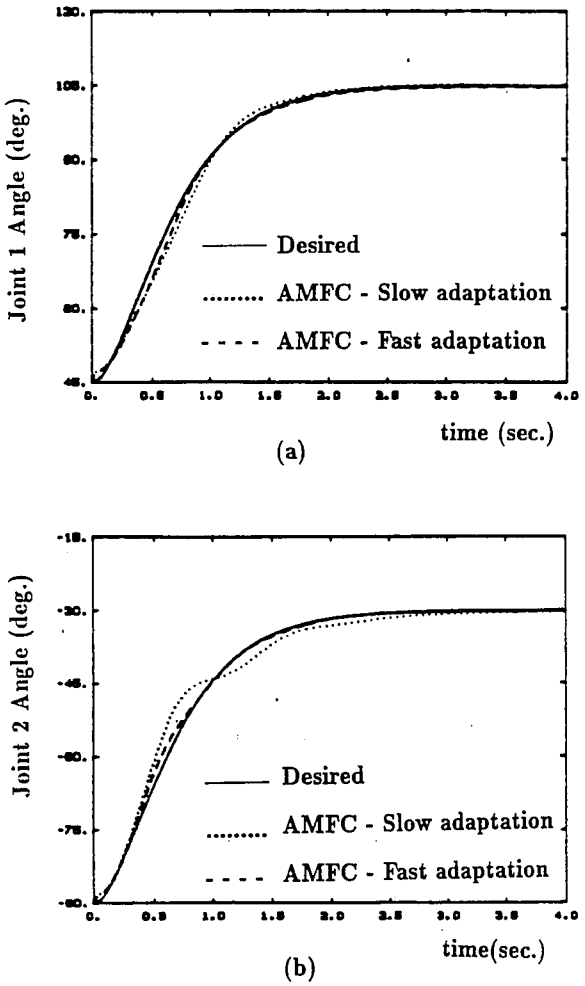

FIG. 10. Joint Angle and Flexible Mode Responses under AMFC Control During the Slow Motion (Fig. 9, curve a).

trial and error. This motion has two properties: 1. Dynamic nonlinearities are not significantly large (Fig. 9, curve (a)); 2. The bandwidth of the desired motion is about ¼ the lowest natural frequency of the arm. The bandwidth of the desired motion, ω_{mi}, is defined as the bandwidth of the reference model which generates the desired motion in response to a step command input ($\mathbf{u}_m$ in Fig. 4).

Since the adaptive controller essentially tries to make the closed loop dynamic behavior equivalent to that of the reference model, the function of ω_{mi} in the nonlinear analysis context is similar to the function of the ω_{r1} in the linear analysis. Clearly Fig. 10a–f show that flexibility of the arm is not significant in terms of joint tracking and settling time of flexible vibrations at the end of motion, which is in agreement with the linear analysis results. When the same system is simulated for motion (b) where $\omega_{mi}/\omega_{cc1} = ½$ and nonlinearities are significant

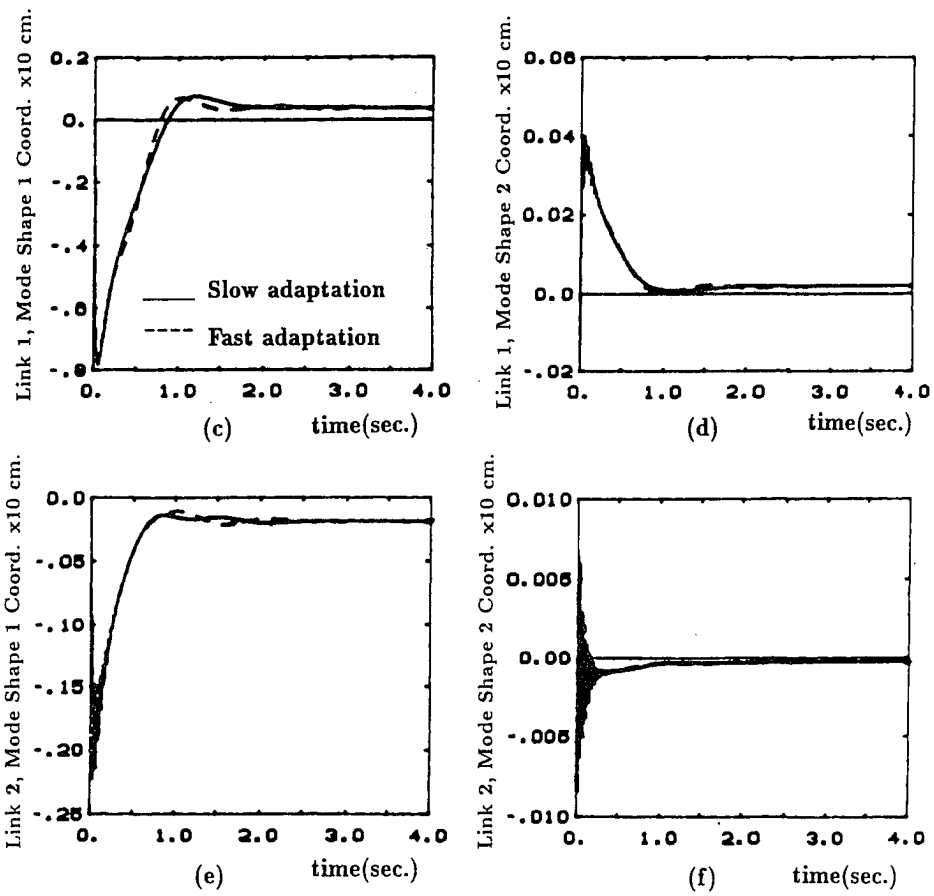

FIG. 10. Cont. Joint Angle and Flexible Mode Responses under AMFC Control During the Slow Motion (Fig. 9, curve a).

(Fig. 9, curve (b)), the response deteriorates. Persistent, lightly damped oscillations occur in joint and flexible mode variables (Fig. 11a–f). The response of the system predictably gets worse for motion (c). The difference here is the nonlinear forces. According to linear analysis results, the performance of the system should be very good and flexibility should not be a problem, for the closed loop bandwidth is not too high ($\omega_{mi}/\omega_{cc1} = \frac{1}{2}$). However, the performance is unacceptably poor and this is due to the dynamic nonlinear forces in high speed gross motion. Therefore, nonlinear effects impose further restrictions on the performance of joint variable feedback controllers in gross motions.

The mechanism through which the nonlinear forces affect the joint controller performance can be described as follows. If the nonlinearities are significant, the adaptive controller automatically adjusts its feedback gains through integral adaptation (equations (4.6c), (4.6d)) to compensate for the tracking errors caused by the nonlinear forces. Increasing the controller gains through the adaptation rule eventually leads to very stiff joints. Linear analysis has shown that very high joint stiffness relative to the flexibility of a given arm results in very lightly

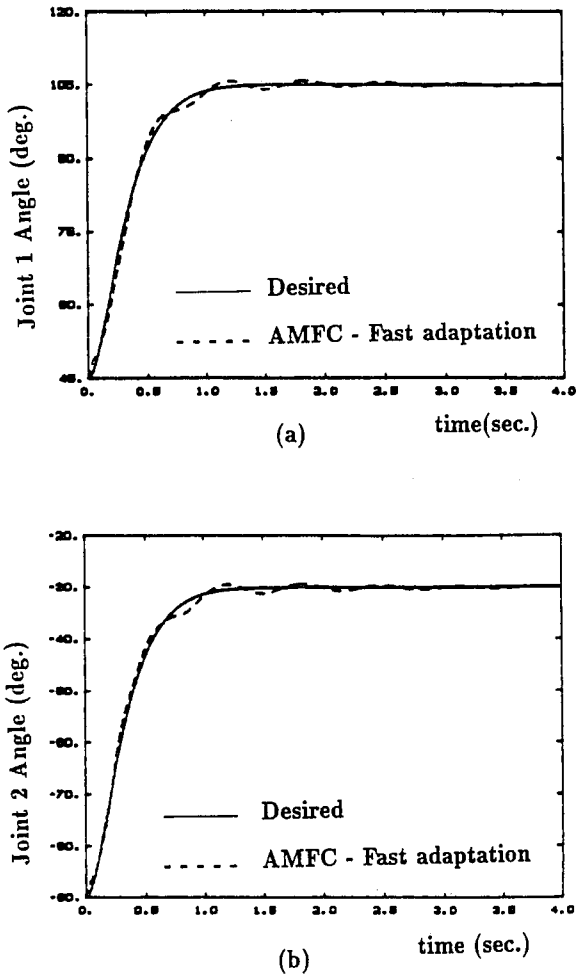

FIG. 11. Joint Angle and Flexible Mode Responses under AMFC Control During the Fast Motion (Fig. 9, curve b).

damped dominant modes (Fig. 5 curves (c), and Fig. 8). Thus, lightly damped dominant modes are generated by the adaptive controller, while it is trying to compensate for the joint tracking errors caused by the large nonlinear forces. It is important to note that this mechanism is valid for the class of model reference adaptive controllers that use integral adaptation only.

VI. Conclusions

In fine motions and gross motions where Coriolis and centrifugal nonlinear forces can be neglected, a given manipulator can be considered rigid if the controller does not attempt to reach closed loop bandwidth more than ½ of ω_{cc1}, the lowest natural frequency of the arm with joints clamped. If the Coriolis and centrifugal forces have comparable magnitudes with gravitational and inertial forces,

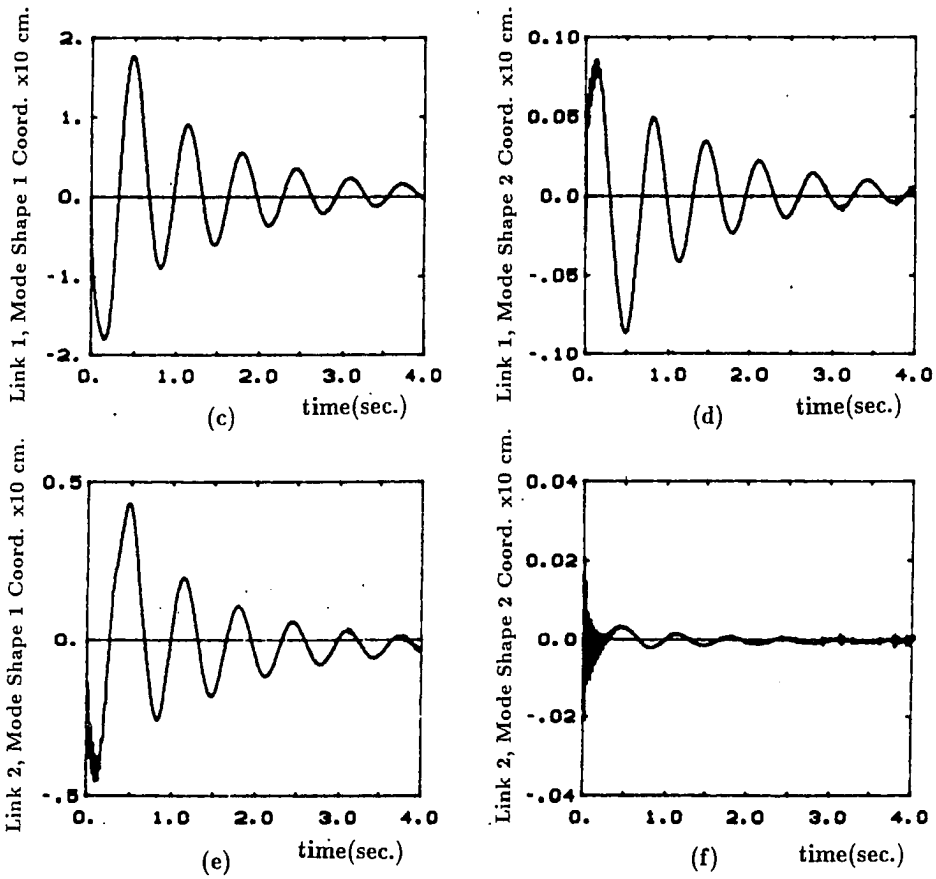

FIG. 11. Cont. Joint Angle and Flexible Mode Responses under AMFC Control During the Fast Motion (Fig. 9, curve b).

the above conclusion is further restricted. In fine motion, the *best* performance of joint variable feedback controllers that can be achieved with damping ratios greater than 0.707 is ⅔ of ω_{cc1} with the appropriate choice of feedback gains. However, it is important to note that the sensitivity of the dominant eigenvalues to the variations of joint feedback gains is highest in the best performance region (Fig. 7f, locations 8, 9, 10, 11). Therefore, it may be difficult to guarantee $(\frac{2}{3})\omega_{cc1}$ closed loop bandwidth due to model inaccuracies. The linear analysis results obtained based on a finite dimensional time domain model agree very well with the results based on infinite dimensional frequency domain models.

The performance of an adaptive control algorithm is limited to a range $(\frac{1}{2}) - (\frac{1}{4})\omega_{cc1}$ in high speed gross motions due to nonlinear effects. If the speed of motion were slow such that dynamic nonlinear effects were negligible, the adaptive controller would achieve a closed loop bandwidth up to $(\frac{2}{3})\omega_{cc1}$ in gross motions as well as in fine motions. If the nonlinearities become significant relative to other dynamic forces, the adaptive controller with integral adaptation automatically increases its feedback gains to compensate for the tracking errors

TABLE 1. Manipulator Dynamic Model Parameters Used in the Analysis

Manipulator model parameters	Value
Geometric properties of uniform, slender links (link 1 and 2 are identical)	
Length of link i (l_i)	2.0 m
Cross-section area of link i (A_i)	7.224×10^{-4} m^2
Cross-section area moment of inertia about z-axis (I_{zi})	7.6190×10^{-9} m^4
Link material properties (Aluminum)	
Mass density (ρ_i)	2.768.8 kg/m^3
Young's modulus of elasticity (E_i)	$7.0 \times 10^{+10}$ Nt/m^2
Resultant link inertial and structural properties	
Mass per unit length ($\rho_i A_i$)	2.0 kg/m
Mass of link i	4.0 kg
Flexural rigidity of link i ($E_i I_{zi}$)	533.33 and 5333.33 Nt–m^2
Lowest natural frequency of the arm (ω_{cc1}) (both joint are locked, and $\theta_2 = 0$)	3.59 and 11.35 rad/sec
Joint inertial parameters	
Joint 1 and 2 masses (m_{j1}, m_{j2})	0.0
Joint 1 and 2 mass moment of inertia about the joint center of mass (J_{j1}, J_{j2})	0.0
Payload inertial properties	
Mass (m_p)	0.0 to 2.0 kg
Mass moment of inertia about the center of mass (J_p)	0.0

caused by the nonlinear forces. As a result, joint stiffness increases and lightly damped dominant modes are generated. Through that mechanism, the nonlinear forces impose further limitations on the performance of model reference *adaptive* joint variable feedback controllers that use *integral adaptation.*

Acknowledgment

This work was supported in part by the National Aeronautics and Space Administration under grant NAG-1-623, and the National Science Foundation under grant MEA-8303539. The authors wish to thank the reviewers for their comments and suggestions that led to improvement of the paper.

References

[1] PAUL, R. P. *Robot Manipulators: Mathematics, Programming, and Control,* The MIT Press, 1983.

[2] LUH, J.Y.S. "Conventional Controller Design for Industrial Robots—A Tutorial," *IEEE Transactions on Systems, Man and Cybernetics,* Vol. SCM-12, No. 3, May–June 1983, pp. 298–316.

[3] BOOK, W.J., MAIZZA-NETO, O., and WHITNEY, D.E. "Feedback Control of Two Beam, Two Joint Systems With Distributed Flexibility," *ASME Journal of Dynamic Systems, Measurement, and Control,* Vol. 97, No. 4, December 1975, pp. 424–431.

[4] HASTINGS, G.G., and BOOK, W.J. "Verification of a Linear Dynamic Model for Flexible Robotic Manipulators," *IEEE Control Systems Magazine,* IEEE Control Systems Society, April 1987.

[5] ALBERTS, T.A., HASTINGS, G.G., BOOK, W.J., and DICKERSON, S.L. "Experiments in Optimal Control of a Flexible Arm with Passive Damping," VPI & SU/AIAA

Symposium on Dynamics and Control of Large Flexible Structures, Blackburg, Virginia, June 1985.

[6] CANNON, R. H., Jr., and SCHMITZ, E. "Initial Experiments on the End-Point Control of a Flexible One-Link Robot," *The International Journal of Robotics Research,* Vol. 3, No. 3, Fall 1984, pp. 62–75.

[7] BALAS, M. J. "Active Control of Flexible Systems," *Journal of Optimization Theory and Applications,* Vol. 25, No. 3, July 1978, pp. 415–436.

[8] SUNADA, W., and DUBOWSKY, S. "The Application of Finite Element Methods to the Dynamic Analysis of Flexible Linkage Systems," *Journal of Mechanical Design,* Vol. 103, 1983, pp. 643–651.

[9] SUNADA, W., and DUBOWSKY, S. "On the Dynamic Analysis and Behavior of Industrial Robotic Manipulators with Elastic Members," *ASME Journal of Mechanisms, Transmissions, and Automation in Design,* Vol. 105, No. 1, March 1983, pp. 42–51.

[10] SHABANA, A. A., and WEHAGE, R. A. "A Coordinate Reduction Technique for Dynamic Analysis of Spatial Substructures with Large Angular Rotations," *Journal of Structural Mechanics,* Vol. 11, No. 3, 1983, pp. 401–431.

[11] NAGANATHAN, G., and SONI, A. H. "Coupling Effects of Kinematics and Flexibility in Manipulators," *The International Journal of Robotics Research,* Vol. 6, No. 1, Spring 1987, pp. 75–84.

[12] SHAHINPOOR, M., and MEGHDARI, A. "Combined flexural-joint stiffness matrix and elastic deformation of a servo-controlled two-link robot manipulator," *Robotica,* Vol. 4, Pt. 4, October–December 1986, pp. 237–242.

[13] HOLLARS, M., and CANNON, R. H. "Initial Experiments on the end-point Control of a Two-link Manipulators with Flexible Tendons," ASME Winter Annual Meeting, Miami Beach, Florida, November 1985.

[14] BOOK, W. J. "Recursive Lagrangian Dynamics of Flexible Manipulator Arms," *International Journal of Robotic Research,* Vol. 3, No. 3, Fall 1984, pp. 87–101.

[15] CETINKUNT, S., and BOOK, W. J. "Symbolic Modeling of Flexible Manipulators," *Proceedings of the 1987 IEEE International Conference on Robotics and Automation, Vol.* 3, March 31–April 3, 1987, Raleigh, North Carolina, pp. 2074–2080.

[16] CETINKUNT, S., and BOOK, W. J. "Symbolic Modeling and Dynamic Simulation of Robotic Manipulators with Compliant Links and Joints," *Journal of Robotics & Computer-Integrated Manufacturing,* Vol. 5, No. 4, 1989, pp. 301–310.

[17] BOOK, W. J., and MAJETTE, M. "Controller Design for Flexible, Distributed Parameter Mechanical Arms Via Combined State Space and Frequency Domain Techniques," *Journal of Dynamic Systems, Measurement, and Control,* Vol. 105, December 1985, pp. 245–254.

[18] CETINKUNT, S., "On Motion Planning and Control of Multi-link Lightweight Robotic Manipulators," Ph.D. Dissertation, The George W. Woodruff School of Mechanical Engineering, Georgia Institute of Technology, November 1987.